

X-ray Twinkles and Pop III Stars

Massimo Ricotti^{1,4*}

¹*Department of Astronomy, University of Maryland, College Park, MD 20742, USA*

11 August 2021

ABSTRACT

Pop III stars are typically massive stars of primordial composition forming at the centers of the first collapsed dark matter structures. Here we estimate the optimal X-ray emission in the early universe for promoting the formation of Pop III stars. This is important in determining the number of dwarf galaxies formed before reionization and their fossils in the local universe, as well as the number of intermediate-mass seed black holes.

A mean X-ray emission per source above the optimal level reduces the number of Pop III stars because of the increased Jeans mass of the intergalactic medium (IGM), while a lower emission suppresses the formation rate of H₂ preventing or delaying star formation in dark matter minihalos above the Jeans mass. The build up of the H₂ dissociating background is slower than the X-ray background due to the shielding effect of resonant hydrogen Lyman lines. Hence, the nearly unavoidable X-ray emission from supernova remnants of Pop III stars is sufficient to boost their number to few tens per comoving Mpc³ by redshift $z \sim 15$.

We find that there is a critical X-ray to UV energy ratio emitted per source that produces a universe where the number of Pop III stars is largest: 400 per comoving-Mpc³. This critical ratio is very close to the one provided by 20 – 40 M_⊙ Pop III stars exploding as hypernovae. High mass X-ray binaries in dwarf galaxies are far less effective at increasing the number of Pop III stars than normal supernova remnants, we thus conclude that supernovae drove the formation of Pop III stars.

Key words: Population III stars – X-rays – SNe – Early Universe

1 INTRODUCTION

The number of first stars (Pop III) per comoving volume that forms in the early universe determines the level and homogeneity of metal pre-enrichment of the intergalactic medium (IGM). Metal pre-enrichment is important for modeling the formation of the first dwarf galaxies and predict the number of pre-reionization fossils in the Local Group (Ricotti & Gnedin 2005; Bovill & Ricotti 2009). There are two main approaches widely used for modeling the formation of the first dwarf galaxies in cosmological simulations: (a) metal enrichment is calculated self-consistently resolving the formation of Pop III stars at $z > 10$ in relatively small (1–4 cMpc³) cosmological volumes (Ricotti et al. 2002a, 2008; Wise & Abel 2008; Wise et al. 2014; Muratov et al. 2013); (b) a metallicity floor (typically $Z \sim 10^{-3} Z_{\odot}$) is introduced everywhere in the IGM in order to run zoom simulations of dwarf galaxies from high-redshift to the present (Gnedin & Kravtsov 2010; Tassis et al. 2012; Christensen et al. 2012;

Kuhlen et al. 2013; Hopkins et al. 2014; Thompson et al. 2014; Wheeler et al. 2015).

The second method is not suited for capturing global feedback loops that might affect the local metallicity floor and the intensity of the radiation backgrounds, which are both important in determining the fraction of dark matter halos that remain dark. However, the self-consistent method in (a) also have limitations:

(i) The gravitational potential of dark matter halos drives the collapse of proto-Pop III stars until the gas becomes self-gravitating at scales of a few AU (Bromm et al. 1999; Abel et al. 2002). Hence, in order to capture the formation of Pop III stars is necessary to resolve the gravitational potential at the center of the minihalos of mass $10^5 M_{\odot}$ with at least several tens of particles. A dark matter resolution of about 100 M_⊙ is required, setting a limit on the cosmological volume that can be simulated (e.g., 512³ simulation with $m_p = 100 M_{\odot}$ has volume of 3 Mpc³).

(ii) On the other hand, the small cosmological volume required to achieve the resolution necessary to resolve Pop III star formation in the smallest dark matter halos, prevents a

* E-mail: ricotti@astro.umd.edu

self-consistent calculation of the radiation backgrounds that are important in determining the number of Pop III stars, especially in underdense regions where local feedback effects are sub dominant.

One can choose to calculate the self-consistent backgrounds even though the simulated volume is too small for numerical convergence, or include a tabulated external background from analytical models. In the first case, as soon as the very first Pop III star is created, the dissociating radiation background jumps from zero to a sufficiently large value to destroy very rapidly all relic H_2 in the IGM (*e.g.*, Ricotti et al. 2002b). For the second choice, often a tabulated background (*e.g.*, Haardt & Madau 2012) is adopted. But in the case of the formation of the Pop III stars at $z = 40 - 10$, the use of backgrounds derived from observations at $z < 10$ is not justified. Hence, both choices are not satisfactory.

In this paper we use simple analytical calculations to estimate self-consistently the number of Pop III stars in the early universe and the radiation background they produce during their short life on the main sequence and by their SN remnants. We also consider other sources of X-rays: accreting intermediated mass black holes (IMBHs), high mass X-ray binaries (HMXRBs) (Xu et al. 2014; Jeon et al. 2014, 2015), and miniquasars. We derive what is the level of X-ray emissivity that maximizes the number of Pop III stars forming at $z \gtrsim 10 - 15$. The basic idea is simple as noted by several authors before (Oh 2001; Venkatesan et al. 2001; Machacek et al. 2003; Ricotti & Ostriker 2004). An X-ray background can both suppress Pop III star formation in the smallest minihalos due to IGM heating (increasing the Jeans mass in the IGM) and promote Pop III star formation by increasing the gas electron fraction in gas collapsed into minihalos and thus promoting H_2 formation via the catalyst H^- .

The number of Pop III stars depends on the minimum dark matter halo mass, M_{cr} , in which a Pop III star can form as a function of redshift; the smaller the critical mass the more numerous the Pop III stars. However, M_{cr} depends on the X-ray background, as explained above, and the H_2 dissociating background (UV in the Lyman-Werner bands); since Pop III stars are responsible for producing the dissociating and X-ray backgrounds, a feedback loop is in play.

The model is presented in § 2 and the results in § 3. The discussion is in § 4, and summary and conclusions are in § 5. We use Planck cosmology ($\Omega_m, \Omega_\lambda, \Omega_b, h, n_s, \sigma_8$) = (0.308, 0.692, 0.0482, 0.678, 0.968, 0.829) (Planck Collaboration et al. 2015).

2 MODEL

The first minihalos that form stars are rare objects in which massive stars and their supernova remnants emit H_2 dissociating radiation in the Lyman-Werner band and hard-UV/soft X-ray radiation (0.2-2 keV), which have long mean free paths. The mean free path of UV hydrogen ionizing radiation is shorter than the distance between Pop III stars until redshift $z \sim 10 - 15$ (neglecting clustering effects) when cosmic H II regions overlap and the UV ionizing background starts dominating the reionization process. In our model we consider only global backgrounds with mean free path longer than the distance between Pop III stars: the H_2 dissociating radiation and a soft X-ray background. In particular,

the inspiration for this paper came from the realization that the mean free path of X-rays is longer than that of the H_2 dissociation radiation that is shielded by resonant Lyman lines in the mostly neutral IGM at $z > 10$ (Haiman et al. 2000; Ricotti et al. 2001). The mean free path of dissociating radiation, hard UV and X-rays are shown in Figure 1 as a function of redshift, in comparison to the particle horizon and the mean distance between halos of mass M_{dm} .

The formation of the first stars in a minihalo is only possible if two conditions are met: the minihalo mass is larger than the Jeans mass (which is $\sim 2 \times 10^8 M_\odot (T_{igm}/10^4 K)^{3/2} [(1+z)/10]^{-3/2}$) in the IGM, and that the gas can cool sufficiently quickly. It is well known that feedback from X-rays can have both a positive or a negative effect on the formation of Pop III stars: intense X-ray emissivity has negative feedback because it heats the IGM, thereby increasing the critical dark matter halo mass that is able to gravitationally attract and condense the IGM gas, thus suppressing Pop III star formation in minihalos. A negligible X-ray emissivity also has a negative impact on Pop III star formation because, although gas can collapse into minihalos, it cannot cool to the molecular form necessary to form stars. H_2 formation is promoted by the reaction $H + H^- \rightarrow H_2 + e^-$, where the formation of the catalyst H^- is maximized for electron fraction $x_e \sim 0.1 - 0.5$ (Ricotti et al. 2001). A weak level of partial ionization by soft X-rays is accordingly ideal to promote H_2 formation and cooling because for $x_e < 0.1$ the photoelectrons deposit most of their energy into secondary ionizations rather than heat. Therefore in this regime the effect of X-rays is to enhance the ionization fraction of the IGM promoting H^- and H_2 formation and cooling, rather than increasing its temperature and Jeans mass that instead would suppress Pop III star formation in small mass minihalos.

In summary, we expect that a weak X-ray emissivity, for instance provided by the first SN remnants, may have the maximum effect at boosting the number of Pop III stars and thus provide metal pre-enrichment and beneficial ionizing radiation to continue star formation in small mass halos formed before reionization.

In order to solve the problem analytically, we make the following assumptions:

a.) We only consider the formation of a single star per minihalo. Simulations have shown that Pop III stars may form in binaries or small multiple systems with a probability of roughly 20% (Turk et al. 2009; Stacy et al. 2010). This scenario can also be considered in our model simply modeling the X-ray emission from possible HMXRB in addition to the total emission from the stars. We will touch on this in § 4.

b.) We assume that all stars are formed from gas of fully primordial composition. Thus, we neglect the contribution to the radiation backgrounds from Pop II stars forming in minihalos externally enriched by powerful supernovae to a critical metallicity prior to collapse (Bromm et al. 2001). However, we include the contribution to the backgrounds from dark matter halos with masses $> 10^8 M_\odot$, which are unaffected by reionization feedback and can cool emitting Lyman- α radiation.

We model the fraction of bolometric energy per source emitted in the X-ray band with the parameter K_X . Therefore the

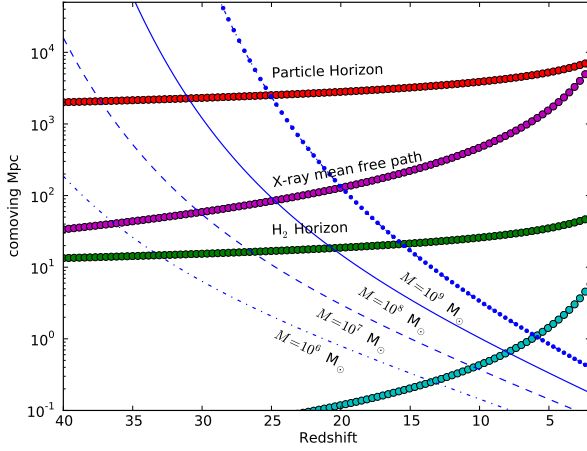


Figure 1. Mean free path of H_2 dissociating radiation (green), hard UV at 54.4 eV (cyan), and soft X-rays at 0.5 keV (magenta) in comparison to the particle horizon (red) and the mean distance between halos of mass $10^6, 10^7, 10^8$ and $10^9 M_\odot$ as indicated by the labels.

limit $K_X = 0$ represent no X-ray emission. The remaining of section describes in detail the analytical model with included physical processes and free parameters.

2.1 Emissivity and backgrounds

We make the simplifying assumption

$$n_{pop3}(z) = n_{halo}(M > M_{cr}, z), \quad (1)$$

where $n_{pop3}(z)$ and $n_{halo}(M, z)$ are the number density of Pop III stars and dark matter minihalos of mass $M > M_{cr}$, respectively. Basically we assume that halos with mass $M < M_{cr}$ remain dark while all halos with mass $M > M_{cr}$ host a Pop III star¹. We derive $M_{cr}(z)$ iteratively at each redshift as explained in § 2.3.

Given the number density of dark matter halos n_{halo} (see Appendix A for a fitting formula based on Press-Schechter formalism), the bolometric emissivity is

$$\epsilon(M_{cr}, z) = n_{halo}(M > M_{cr}, z) L'_* f_{duty} \quad (2)$$

where $f_{duty} = t'_{on}/t_H(z)$ is the fraction of Hubble time the sources are emitting radiation at luminosity L'_* and t'_{on} is the typical lifetime during which a star emits radiation before leaving the main sequence and exploding as a SN or Hypernova. Here we adopt parameters $L'_* = 10^{40}$ ergs/s and $t'_{on} = 2$ Myr typical of a $100 M_\odot$ Pop III star, or a total emitted energy per source $E_{pop3} = L'_* t'_{on} = 6 \times 10^{53}$ ergs. In general, the values of t_{on} and L_* depend on the initial mass function (IMF) of Pop III stars. Very massive stars ($> 100 M_\odot$) emit near the Eddington limit, thus $L_* \approx 10^{40}$ ergs/s ($M_*/100 M_\odot$). Since we have assumed

¹ When a large fraction of dark matter halos fail to host galaxies, we expect a large scatter in the mass-to-light ratio due to local environmental effects. Here we neglect these local variations and we instead focus on how the global radiation backgrounds affect star formation in isolated minihalos.

Table 1. List of free parameters in the model.

Parameter	Explanation
$K_{LW} \equiv \frac{E_{LW}}{6 \times 10^{53} \text{ ergs}}$	E_{LW} is the mean energy emitted from Pop III stars per minihalo in the Lyman-Werner bands.
$K_X \equiv \frac{E_X}{6 \times 10^{53} \text{ ergs}}$	E_X is the mean energy emitted per minihalo in the X-ray bands (0.2 – 2 keV). Note that $\beta_X \equiv K_X/K_{LW}$ is a derived parameter.
$T_0 \equiv \frac{\Gamma_{HI}}{k_B \zeta_{HI}}$	Characteristic spectral temperature of the sources, proportional to the ratio of the photo-heating to photo-ionization rate. It depends on the source spectrum modified for ISM absorption.

a fixed L'_* and t'_{on} , typical of $100 M_\odot$ Pop III stars, we can model an arbitrary IMF by adjusting two of the three free parameters in our model: $K_{LW} \equiv L_{LW} t_{on}/E_{pop3}$, the mean energy emitted per source (or, equivalently, per minihalo) in the Lyman-Werner bands, and $K_X \equiv L_X t_{on}/E_{pop3}$, the mean energy per source (minihalo) in the soft X-ray band. Thus, the emissivity in a given frequency band is $\epsilon_{band}(M, z) = K_{band} \epsilon(M, z)$. We refer to § 4 for details on the typical values of K_{LW} and K_X for different IMFs of Pop III stars and X-ray sources (*e.g.*, SNe, Hypernovae, HMXRBs). For reference, the free parameters in our model are listed in Table 1.

In addition, we include the rise of galaxies forming in halos with masses $> 10^8 M_\odot$, that are not subject to either thermal or cooling feedback (since their virial temperature is $> 10^4$ K, the gas is collisionally ionized and can cool by Lyman- α emission). Note that $M_{cr} < 10^8 M_\odot$ in all cases. We thus add to the emissivity in the X-ray and Lyman-Werner bands the term

$$\epsilon_{band}(> 10^8 M_\odot, z) = K_{UV} n_{halo}(10^8 M_\odot, z) L'_* f_{duty}, \quad (3)$$

where $K_{UV} = 1$ is chosen to reheat and reionize the IGM at $z \sim 5-6$. These “Lyman- α cooling” galaxies are thought to be the primary agents of hydrogen reionization (Ricotti et al. 2002b; Robertson et al. 2015) but have negligible effect on the IGM, the number of Pop III stars and the radiation backgrounds at $z > 15$. The decline of the number of Pop III stars and the radiation backgrounds they produce observed in our models at $z \lesssim 10$ is due to the rise of this more massive population of galaxies.

Given the specific emissivity, the mean specific intensity of the background $J_\nu \equiv J_0 g_\nu$ is

$$4\pi J_\nu = \min(\lambda_\nu, ct_H) \epsilon_\nu(M_{cr}, z), \quad (4)$$

where $\lambda_\nu = (\sigma_\nu n_{HI})^{-1}$ is the photon mean free path. When the mean free path is smaller than the particle horizon (for instance for photon energies < 2 keV in the mostly neutral IGM at $z > 10$), we have $J_\nu \propto \epsilon_\nu/n_H \sigma_\nu$. Thus, in this case the ionization and heating rates [see Eqs. (7)-(8)] become independent of the ionization cross section because all photons are eventually absorbed before being significantly redshifted.

2.2 Electron fraction and temperature of the IGM

In order to know whether a minihalo is able to form a Pop III star we need to determine whether the gas in the

IGM can condense into the gravitational potential of minihalos of mass M . We thus need to calculate the Jeans mass of the IGM and therefore its temperature evolution. A gas of primordial composition in minihalos of mass $< 10^8 M_\odot$ can cool and form stars only if a sufficient amount of H_2 is formed in the minihalo. As explained above, the formation of molecular hydrogen is catalyzed by the ion H^- formed by the reaction $H + e^- \rightarrow H^- + \gamma$, whose rate depends on the ionization fraction of the gas. Both temperature and ionization fraction are determined by the radiation backgrounds, that in turn are proportional to the number of minihalos hosting a Pop III star, establishing a feedback loop.

The evolution of the electron fraction and temperature of the IGM depend on the ionizing radiation background by the following equations:

$$\frac{dx_e^{\text{igm}}}{dt} = f_i \zeta_{HI}, \quad (5)$$

$$k_B \frac{dT^{\text{igm}}}{dt} = f_h \Gamma_{HI}. \quad (6)$$

where,

$$\zeta_{HI} = 4\pi J_0 \int \frac{d\nu}{h\nu} g_\nu \sigma_\nu, \quad (7)$$

$$\Gamma_{HI} = 4\pi J_0 \int d\nu g_\nu \sigma_\nu \equiv k_B T_0 \zeta_{HI}, \quad (8)$$

are the ionization and heating rates, respectively. The characteristic temperature T_0 depends only on the spectrum g_ν of the source modified for ISM absorption, and is the third free parameter in the model. Integrating the equations above we obtain:

$$x_e^{\text{igm}} = f_i \frac{\Gamma_{HI} t_H}{k_B T_0}, \quad (9)$$

$$k_B T^{\text{igm}} = f_h \Gamma_{HI} t_H, \quad (10)$$

where $\Gamma_{HI} = K_X \epsilon / n_{HI}$. Thus, the temperature of the IGM can be easily determined from the electron fraction. In summary:

$$x_e^{\text{igm}}(M_{\text{cr}}, z) = f_i \frac{K_X \epsilon(M_{\text{cr}}, z)}{k_B T_0} \frac{t_H}{n_H}, \quad (11)$$

$$T^{\text{igm}}(M_{\text{cr}}, z) = T_0 x_e^{\text{igm}} \frac{f_h}{f_i}, \quad (12)$$

where the functions $f_h(x_e)$, $f_i(x_e)$, given in appendix B, account for the effect of secondary ionization from fast photoelectrons (Shull & van Steenberg 1985; Valdés & Ferrara 2008). A minimum $x_e^{\text{igm}} = 10^{-4}$, due to the residual ionization after recombination (*e.g.*, Tegmark et al. 1997), is set as a ionization floor². Similarly, the temperature floor of the IGM in absence of heating sources is given by the cosmic adiabatic expansion after radiation-gas thermal decoupling at $z \sim 100$: $T^{\text{igm}} = 300 \text{ K} [(1+z)/100]^2$.

The X-ray and Lyman-Werner backgrounds can also be

² There are no other processes setting a floor value for the electron fraction at high- z other than exotic sources like primordial BHs (Ricotti et al. 2008) or decaying dark matter (Mapelli et al. 2006). At lower redshifts escaping UV radiation may produce short lived bubbles of ionized gas that after recombining leave behind long-lived relic H II regions of partially ionized gas (Hartley & Ricotti 2016). Inside those relic H II regions Pop III star formation might be enhanced, but we have neglected this effect.

derived as a function of T^{igm} . For the Lyman-Werner band the mean free path in the mostly neutral IGM is about 150 times smaller than the particle horizon due to the shielding effect of resonant Lyman- α lines (see Fig. 12 in, Ricotti et al. 2001). Thus, from Equation (4) and $K_X \epsilon = \Gamma_{HI} n_H = k_B T^{\text{igm}} / (f_h t_H)$, we get:

$$4\pi J_{LW} = K_{LW} \epsilon(M_{\text{cr}}, z) \frac{ct_H}{150} = \frac{K_{LW}}{K_X} \frac{cn_H(z)}{150 f_h} k_B T^{\text{igm}}. \quad (13)$$

2.3 Formation of Pop III stars and feedback loop

The formation of Pop III stars in a minihalo of mass M is only possible if these two conditions are met:

(i) $T_{\text{vir}}(M, z) > T^{\text{igm}}(M_{\text{cr}}, z)$: the dark matter halo mass is larger than Jeans mass of the IGM. This condition is satisfied for dark matter halo masses $M > M_{\text{cr}}^i$.

(ii) $t_{\text{cool}}(M, z) < t_H(z)$: the virialized gas inside dark matter halos of mass M cools in less than the Hubble time. This condition is satisfied for dark matter halo masses $M > M_{\text{cr}}^{ii}$.

For a given temperature of the IGM, T^{igm} , only halos with virial temperature $T_{\text{vir}} > T^{\text{igm}}$ can condense gas from the IGM. A gas at the virial temperature in hydrostatic equilibrium in the potential of a dark matter halo with virial radius r_{vir} , has a gas core radius $r_c \sim (0.22/c) r_{\text{vir}}$ with gas overdensity $\delta_c \sim 2000$ (Ricotti 2009). Here we have assumed halo concentration parameter $c = 5$. A hot IGM increases the minimum dark matter halo mass that is able to form stars, M_{cr}^i , thus reduces the number of X-ray sources and the X-ray background. But a lower X-ray background translates into lower IGM temperature. Clearly, this is the first feedback loop in play.

The second condition is:

$$t_{\text{cool}} = \frac{k_B T_{\text{vir}}}{\delta_c n_H x_{H_2} \Lambda(T_{\text{vir}})} < t_H(z), \quad (14)$$

where $\Lambda(T)$ [erg cm³ s⁻¹], given in Appendix B, is from (Galli & Palla 1998). Condition (ii) sets a minimum x_{H_2} for collapse. The H_2 abundance depends on the formation of H^- and is regulated by the gas temperature in virialized halos, $T_{\text{vir}}(M, z)$, as well as the dissociating radiation background and the electron fraction in the halo according to the equation:

$$x_{H_2}(M, z) = n_e \frac{k_1(T_{\text{vir}})}{k_2(G_{LW})} \left(1 + \frac{N_{H_2}}{10^{14} \text{ cm}^{-2}} \right)^{0.75}, \quad (15)$$

where $G_{LW} \equiv J_{LW} / (1.6 \times 10^{-3} \text{ erg/s/cm}^2)$. The H^- formation rate, k_1 , and the H_2 dissociation rate, k_2 , are given in Appendix B. We have also included the effect of H_2 self-shielding, that is important for H_2 column densities $N_{H_2} \equiv r_c n_{H_2} > 10^{14} \text{ cm}^{-2}$, where r_c is the core radius of the gas in hydrostatic equilibrium in the dark matter halo.

Inside dark matter halos (with gas overdensity δ_c) the electron fraction differs from the value in the IGM because of the larger recombination rate. Thus, the equilibrium electron fraction inside dark matter halos is:

$$n_e = \delta_c n_H \sqrt{x_e^{\text{igm}} R} \quad (16)$$

$$R = \min(x_e, t_{\text{rec}}/t_H). \quad (17)$$

Thus, condition (ii) sets a feedback loop that regulates the number of Pop III stars as follows: lowering the minimum halo mass hosting Pop III stars $M_{\text{cr}}^{\text{ii}}$ with respect to the feedback regulated value increases the number of sources producing a higher electron fraction but also a higher dissociating background. The H_2 formation rate and the gas temperature (equal to the halo virial temperature) are both reduced resulting in a cooling time longer than the Hubble time. Thus $M_{\text{cr}}^{\text{ii}}$ needs to increase to satisfy condition (ii).

In order to satisfy both conditions (i) and (ii) the critical mass must be

$$M_{\text{cr}}(z) = \max[M_{\text{cr}}^{\text{i}}(z), M_{\text{cr}}^{\text{ii}}(z)]. \quad (18)$$

When the critical mass is set by the cooling condition (*i.e.*, when $M_{\text{cr}} = M_{\text{cr}}^{\text{ii}}$ and $M_{\text{cr}}^{\text{i}} < M_{\text{cr}}^{\text{ii}}$), increasing the X-ray emissivity K_X produces higher electron fraction and H_2 fractions in dark matter halos, reducing $M_{\text{cr}}^{\text{ii}}$, thus increasing the number of Pop III stars. At the same time increasing K_X increases the IGM temperature and the Jeans mass in the IGM. Thus M_{cr}^{i} increases approaching $M_{\text{cr}}^{\text{ii}}$. The maximum number of Pop III stars at any given redshift (for a fixed K_{LW}) is obtained for a value of $K_X = K_X^{\text{cr}}$ that makes the critical masses from conditions (i) and (ii) equal to each other (*i.e.*, $M_{\text{cr}}^{\text{i}} = M_{\text{cr}}^{\text{ii}}$). For $K_X > K_X^{\text{cr}}$ the critical mass is set by the Jeans condition ($M_{\text{cr}} = M_{\text{cr}}^{\text{i}}$ and $M_{\text{cr}}^{\text{ii}} < M_{\text{cr}}^{\text{i}}$), thus increasing K_X leads to a higher Jeans mass in the IGM, a higher M_{cr} and reduces the number of Pop III stars.

3 RESULTS

The initial mass function for the first stars and the nature of their relics are very uncertain, so we start by examining three cases that illuminate the range of available parameter space. We will keep the ultraviolet luminosity and spectrum of the sources fixed adopting $K_{\text{LW}} = 10^{-2}$ and $T_0 = 2 \times 10^5$ K (typical of $\sim 40 M_{\odot}$ Pop III stars) and vary K_X considering the cases: i) low X-ray energy per source (*e.g.*, the baseline X-ray emission from normal SN explosions); ii) moderate X-ray energy (*e.g.*, if Pop III stars explode as hypernovae); iii) strong X-ray energy per source (*e.g.*, produced by an hypothetical population of miniquasars or accreting intermediate mass black holes).

In Figure 2 we show the results for the three sets of runs. The top two panels show the evolution as a function of redshift of the critical mass M_{cr} for Pop III formation and the number of Pop III stars per comoving Mpc³. The two panels in the middle show the evolution as a function of redshift of the electron fraction, x_e^{igm} , and temperature, T^{igm} , of the IGM. The bottom two panels show the evolution of the soft X-ray background at 0.5 keV, J_X , and the H_2 dissociating background in the Lyman-Werner bands, J_{LW} .

For the low X-ray energy case ($K_X = 10^{-5}$, red lines in Figure 2), the X-ray background has a small effect on the evolution of the ionization fraction (x_e^{igm}) and temperature of the IGM (T^{igm}) until redshift $z \lesssim 15$, when halos with mass $> 10^8 M_{\odot}$ start dominating the UV and X-ray emission. The Jeans mass in the IGM (*i.e.*, the minimum mass that can collapse gravitationally) is small but the gas collapsed into minihalos does not cool and therefore cannot form stars because the H_2 cooling time is longer than the Hubble time, which at $z = 15$ is 272 Myr. In this model the

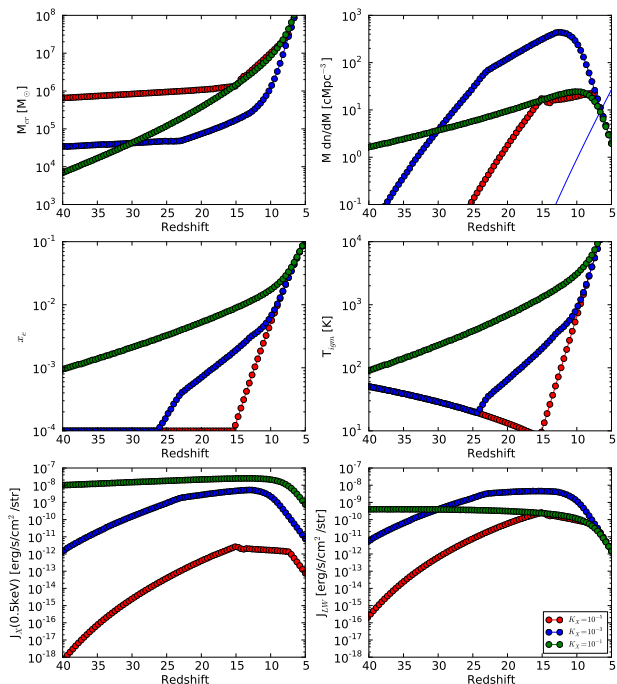


Figure 2. Simulations of Pop III star formation and its effect on the IGM for three different models differing for the X-ray emissivity of the sources: (Top left.) Evolution of the critical mass M_{cr} for Pop III star formation as a function of redshift, z . (Top right.) Number of Pop III stars per comoving Mpc as a function of z . The thin blue line in this panel shows the number of Lyman- α cooling halos ($M > 10^8 M_{\odot}$). (Middle left.) Electron fraction x_e^{igm} , and (middle right) temperature of the IGM, T^{igm} , as a function of z . The bottom panels show the evolution of the X-ray background (bottom left) and H_2 dissociating background (bottom right). The simulation parameters are $T_0 = 2 \times 10^5$ K, $K_{\text{LW}} = 10^{-2}$ and $K_X = 10^{-5}$ (red), 10^{-3} (blue), and 10^{-1} (green). See the text for the meaning of the free parameters T_0 and K_{LW} .

minimum halo mass in which Pop III stars can form (M_{cr}) is the largest of the three models, and the total number of Pop III stars at $z \sim 15$ (and the radiation background they produce) is the lowest among the three models. In all the runs at $z < 15$ Lyman- α cooling halos with $M > 10^8 M_{\odot}$, which are not subject to the feedback loop, start to dominate the radiation emissivity. The reheating of the IGM and Lyman-Werner background produced by these halos start suppressing the formation of Pop III stars. However, several simplifying assumptions in our model become increasingly unrealistic at $z < 10 - 15$. For instance, metal enrichment from powerful winds in these halos is expected to suppress Pop III star formation.

In the model with strong X-ray energy per source ($K_X = 10^{-1}$, green lines), the ionization fraction and temperature of the IGM rise rapidly. The minimum mass of dark matter halos in which Pop III star can form (M_{cr}) coincides with the IGM Jeans mass, which increases rapidly with time. Thus, the number of Pop III stars is relatively large at high-redshift but does not increase significantly with time. The intensity of the X-ray background J_X is the highest with respect to the three models and rather constant with redshift, while

the dissociating background J_{LW} is the highest at high- z but becomes lower than in the intermediate model with decreasing redshift.

The model with moderate X-ray energy ($K_X = 10^{-3}$, blue lines) maximizes the number of Pop III stars per unit volume at $z \sim 15$. The maximum number of Pop III stars is obtained when the critical halo mass in which gas can cool in a Hubble time equals the Jeans mass of the IGM. The background in the Lyman-Werner band is the highest and the X-ray background is also very close to the highest among the three models. The maximum number of Pop III stars is reached around redshift $z \sim 15$, before the radiation by normal stars dominates the background.

In Figure 3 we show the maximum number of Pop III stars per comoving Mpc^3 (reached at redshift z^{max}), as a function of K_X (left panel), and as a function of $\beta_X \equiv K_X/K_{LW}$ (right panel) for different values of K_{LW} as shown in the legend. For low values of K_X , the maximum number of Pop III stars, $n_{pop3}(z^{max})$, increases as β_X increases (achieved by either increasing K_X or decreasing K_{LW}). This is the regime where the number of Pop III stars is limited by the H_2 formation rate and thus the ability of the gas collapsed inside minihalos to cool in less than a Hubble time. For higher K_X the number of Pop III stars is independent of K_{LW} and decreases with increasing K_X . In this regime the number of Pop III stars is limited by the heating of the IGM, which prevents gas from collapsing into minihalos.

The number of Pop III stars per cMpc^3 is approximated by a broken power:

$$n_{pop3} = 6 \text{ cMpc}^{-3} \times \begin{cases} \left(\frac{\beta_X}{2 \times 10^{-4}}\right)^{0.15} & \text{if } \beta_X < 2 \times 10^{-4} \\ \left(\frac{\beta_X}{2 \times 10^{-4}}\right)^{0.73} & \text{if } 2 \times 10^{-4} < \beta_X < \beta_X^{\text{cr}} \\ K_X^{-0.73} & \text{if } \beta_X > \beta_X^{\text{cr}}, \end{cases} \quad (19)$$

and reaches its maximum value

$$n_{pop3}^{max} = 430 \text{ cMpc}^{-3} \left(\frac{K_{LW}}{10^{-2}}\right)^{-0.365}, \quad (20)$$

when the critical mass for cooling and the IGM Jeans mass coincide. This happens for $\beta_X = \beta_X^{\text{cr}} = 0.01 K_{LW}^{0.5}$ or equivalently, $K_X = K_X^{\text{cr}} = 0.01 K_{LW}^{0.5}$.

For our fiducial choice $K_{LW} = 10^{-2}$, typical of $40 M_\odot$ Pop III stars (see § 4), we find $\beta_X^{\text{cr}} = 0.1$ (or $K_X^{\text{cr}} = 10^{-3}$). We will show in the next section that this corresponds best to a population of $\sim 40 M_\odot$ stars exploding as hypernovae (see yellow circles in the figure for the parameters of different X-ray sources). We also find that the contribution of HMXBs corresponds to a ratio $\beta_X = 10^{-4}$ (see § 4) and therefore they play no role in either suppressing or enhancing the formation of Pop III star.

4 DISCUSSION

We have not discussed yet the type of sources that can provide the level of X-ray and Lyman-Werner emissivity able to boost or suppress the formation of Pop III stars. Our results are given in terms of the dimensionless energies emitted by each source in the X-ray and Lyman-Werner bands: K_X and K_{LW} , respectively. The normalization we adopted (see

§ 2.1) is typical of $100 M_\odot$ Pop III stars: $E_{pop3} = L'_* t'_{on} = 10^{40} \text{ erg/s} \times 2 \text{ Myr} = 6 \times 10^{53} \text{ erg}$. Hence, as discussed before, the value of $K_{LW} \equiv E_{LW}/(6 \times 10^{53} \text{ ergs})$, depends on the IMF of Pop III stars. We consider three representative cases (Helgason et al. 2015):

(i) **Very massive Pop III stars ($100 - 500 M_\odot$).** They emit close to the Eddington limit and a significant fraction of their bolometric luminosity is in the UV bands: the luminosity per solar mass in stars in the Lyman-Werner bands is $2.7 \times 10^{37} \text{ erg/s}$ and $t_{on} = 2 \text{ Myr}$, hence:

$$K_{LW} = 2.7 \times 10^{-1} \left(\frac{M_*}{100 M_\odot}\right).$$

(ii) **Massive Pop III stars ($10 - 40 M_\odot$).** In this mass range the luminosity per solar mass is sub-Eddington: $L_{LW} = 2.7 \times 10^{36} \text{ erg/s}$ and $t_{on} = 2 \text{ Myr}$, hence

$$K_{LW} = 10^{-2} \left(\frac{M_*}{40 M_\odot}\right).$$

(iii) **Metal poor stars with Kroupa IMF.** The luminosity per solar mass is sub-Eddington but the lifetime of the stars is longer: assuming masses between 0.1 and $100 M_\odot$ with metallicity of $Z=0.0004$, the mean luminosity per star (which has mean mass of $0.64 M_\odot$) is $L_{LW} = 0.64 \times 10^{36} \text{ erg/s}$, and $t_{on} = 10 \text{ Myr}$. Hence, still assuming one star per halo, we estimate:

$$K_{LW} = 3.2 \times 10^{-4}.$$

In the following subsections we estimate the values of K_X and β_X for different X-ray emitting sources, starting from SN explosions and SN remnants of Pop III stars. To estimate β_X we assume K_{LW} in case (ii).

4.1 Supernova remnants of Pop III stars

The first SNe are a nearly unavoidable outcome of the formation of the Pop III stars (unless all Pop III stars have masses $M_* > 250 M_\odot$ and collapse into BHs without exploding (Heger & Woosley 2002)). Thus, SNe set a minimum floor for the X-ray emissivity. The assumption that the X-ray and Lyman-Werner emissivity are directly proportional to the number of Pop III stars is clearly satisfied in this case.

Normal SNe with standard energy of the explosion, $E_{SN} = 10^{51} \text{ erg}$, emit mostly soft X-rays in band $0.2 - 2 \text{ keV}$. The X-ray luminosity from the hot gas in the SN cavity is about $L_X = 10^{37} \text{ erg/s}$, and it emits for about $t_{on} = 10^4 \text{ yr}$ before cooling. Thus, the total energy in the soft X-ray bands is $E_{SNR} = 3 \times 10^{48} \text{ erg}$ (Lopez et al. 2011). The supernova explosion itself also emits in the X-ray bands with peak luminosity $L_X = 10^{42} \text{ erg/s}$ lasting about $t_{on} = 1 \text{ month}$. Thus, the total emitted energy in X-rays is comparable to the remnant's energy: $E_{SN} \approx 2.6 \times 10^{48} \text{ erg}$. The total energy emitted in the soft X-ray band from each Pop III SN explosion (independently of the Pop III mass as long as $M_* > 8 M_\odot$) is $E_{X,tot} = E_{SN} + E_{SNR} \approx 6 \times 10^{48} \text{ erg}$, corresponding to $K_X = 10^{-5}$. Hence, for the fiducial K_{LW} we find

$$\beta_X(\text{SNe}) = 10^{-3} \left(\frac{M_*}{40 M_\odot}\right)^{-1}. \quad (21)$$

We speculate that if a fraction of Pop III stars explode as hypernovae (Umeda & Nomoto 2003) or pair-instability

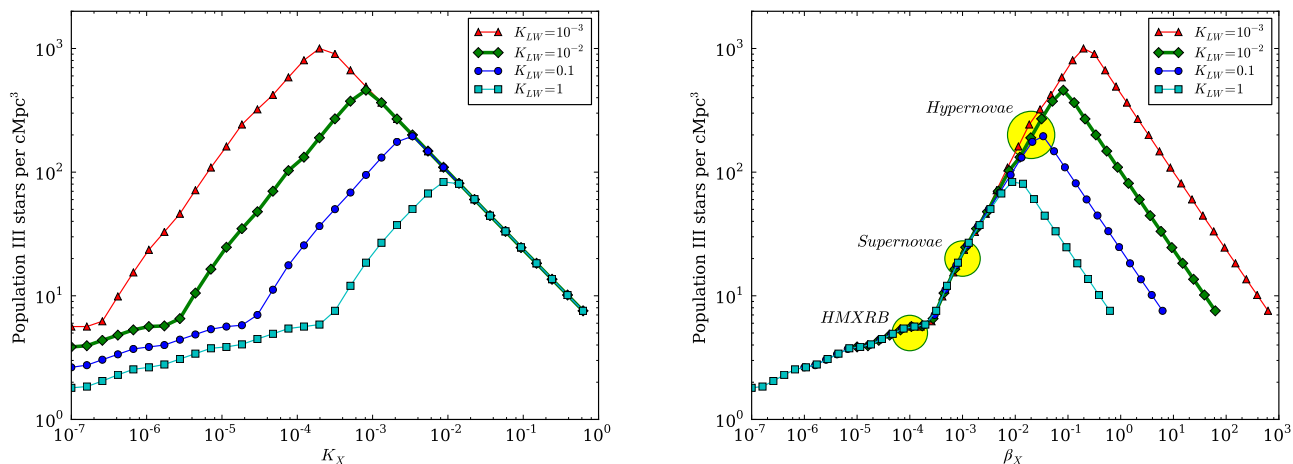


Figure 3. (Left) Maximum number of Pop III stars per comoving Mpc^3 forming at a given redshift (around $z \sim 10 - 13$) as a function of K_X , for different values of K_{LW} , as shown in the legend. The parameters K_{LW} and K_X , are the mean UV (in the Lyman-Werner band) and soft X-ray energy emitted by each source in units of 6×10^{53} ergs (roughly the bolometric energy emitted over its lifetime by a Pop III star of $100 M_\odot$). (Right) Maximum number of Pop III stars per comoving Mpc^3 (forming at a given redshift) as a function of $\beta_X \equiv K_X/K_{LW}$, for different values of K_{LW} . The yellow circles show approximate values of β_X for different X-ray sources as indicated by the labels: high mass X-ray binaries (HMXRBs), supernovae and hypernovae.

SNe (PISNe), that are about 10 to 100 times more energetic than normal SNe, then $K_X \sim 10^{-3} - 10^{-4}$ and

$$\beta_X(\text{Hypernovae}) \sim 10^{-1} - 10^{-2}, \quad (22)$$

depending on the details of the emitted energy and the fraction of Pop III stars that explode as hypernovae. Thus, an exciting insight from this study is the following: if a non-negligible fraction of Pop III stars end their lives as hypernovae, the soft X-rays from their remnants and explosions is sufficient to promote the formation of Pop III stars to about 400 per cMpc^3 , that is near the maximum value found for any choice of K_X and the assumed IMF of Pop III stars.

4.2 High mass X-ray binaries (HMXRB)

The X-ray emission does not come directly from Pop III stars in this case but from normal dwarf galaxies with more than one star. Thus, we have to make the additional assumption that the emission from normal galaxies is proportional to the number of minihalos hosting a Pop III star.

To estimate the X-ray emission from low metallicity HMXRB we use the empirical relationship (Fragos et al. 2013):

$$L_X = 2.4 \times 10^{39} \text{ erg/s} \left(\frac{\text{SFR}}{1 M_\odot/\text{yr}} \right) \text{ at } 0.5\text{-}2 \text{ keV}. \quad (23)$$

HMXRB emit more significantly in the hard X-ray band than the soft X-ray band. The IGM is optically thin to hard X-rays even at $z > 10$, thus a significant fraction of the X-ray photons are not available for ionization or heating of the IGM until they get redshifted to lower energies at $z \sim 2 - 3$ (Ricotti & Ostriker 2004; Ricotti et al. 2005). The same normal dwarf galaxies that host HMXRB have stars that radiate in the Lyman-Werner bands: for a $\text{SFR} = 1 M_\odot/\text{yr}$ the luminosity estimated using Starburst 99 is $L_{LW} = 3 \times 10^{43} \text{ erg/s}$ (roughly in agreement with the values given in § 4).

For the weak X-ray irradiation regime, $\beta_X < \beta_X^{\text{cr}}$, the number of Pop III stars depends only on the ratio β_X of X-ray to the Lyman-Werner energy emitted by each source. Assuming that normal galaxies dominate the X-ray emission, the results are independent of the level of SFR in early dwarf galaxies because both L_X from HMXRB and L_{LW} are proportional to the SFR. Thus, we find

$$\beta_X(\text{HMXRB}) = 10^{-4}, \quad (24)$$

that is lower than the contribution from normal SNe from Pop III stars, thus can be neglected.

Our result is not in contradiction with simulation results from Xu et al. (2014); Jeon et al. (2014, 2015). Those studies focus on local effects (*i.e.*, Pop III star formation and heating of the IGM in a small-box simulation) produced by a pre-calculated X-ray background from HMXRBs in low-metallicity dwarf galaxies (not coupled to star formation in the box). Our study instead focuses on global effects (*i.e.*, in large volumes) at high redshifts when the X-ray background can be calculated self-consistently within a feedback loop in which the number of X-ray sources producing the background is determined by the intensity of the background they produce. However, our model is unable to capture local effects and its validity starts to break down at redshifts $z < 10$ when halos with masses $> 10^8 M_\odot$ and galaxies forming predominantly Pop II stars (due to metal pre-enrichment) become prevalent and dominate the buildup of radiation backgrounds.

4.3 Moving IMBHs in the ISM of primordial galaxies

If Pop III stars produce IMBH remnants, these can accrete gas from the ISM and radiate in normal dwarf galaxies after the minihalos hosting Pop III stars merge to form more massive halos. The emission from IMBH is thus propor-

tional to the number of Pop III stars per unit volume as required by our model. An IMBH of mass $100 M_\odot$, moving at $v \sim 20\text{--}30$ km/s in an ISM of density 10^4 cm^{-3} , ISM typical for early dwarf galaxies of mass $M_{dm} > 10^7\text{--}10^8 M_\odot$, emits continuously (without periodic luminosity burst typical of stationary accreting BHs) at about 3% of the Eddington rate: $L_X \approx 3 \times 10^{38}$ erg/s, $t_{on} \approx t_H(z=10) \approx 400$ Myr (Park & Ricotti 2013). Thus, if a fraction (in number), f_{imbh} , of the remnants of Pop III stars is a $100 M_\odot$ IMBH accreting from the ISM at this rate we find (assuming the fiducial $K_{LW} = 10^{-2}$ for $40 M_\odot$ Pop III stars):

$$\beta_X(\text{IMBH}) = 10^{-2} \left(\frac{f_{imbh}}{1.6 \times 10^{-5}} \right). \quad (25)$$

4.4 Miniquasars

Similarly to the case of IMBH, if a fraction of Pop III stars produce massive BHs, the emission of miniquasars is proportional to the number of Pop III stars, as required by the model. Here we estimate the contribution to the soft X-ray (mean) luminosity of the first objects from the emission of rare miniquasars in the most massive halos. Let's assume as an example $10^5 M_\odot$ miniquasars accreting at near the Eddington rate $L_{mqso} = 10^{43}$ erg/s ($M_{mqso}/10^5 M_\odot$). For this mass BHs, based on theoretical arguments (Park & Ricotti 2011, 2012), the period between bursts is about 10 Myr and the duty cycle 6%, also in agreement with observations at lower redshift (*e.g.*, Steidel et al. 2002). Thus, during $t_H(z=10) \approx 400$ Myr the emission time is $t_{on} = 24$ Myr. Assuming a fraction (in number) of miniquasars per Pop III stars, f_{mqso} , and comparing to the Lyman-Werner luminosity from $40 M_\odot$ Pop III stars, we get

$$\beta_X(\text{miniQSO}) = 10^{-2} \left(\frac{f_{mqso}}{8 \times 10^{-9}} \right) \left(\frac{M_{mqso}}{10^5 M_\odot} \right), \quad (26)$$

meaning that one miniquasar of $10^5 M_\odot$ per 10^8 Pop III stars (or, assuming about 100 Pop III stars per cMpc^3 , one miniquasar per about 10^6 cMpc^3) would boost the formation of Pop III stars to near its maximum.

5 SUMMARY AND CONCLUSIONS

A low level of X-ray emission in the early universe, although has a negligible effect on reionization and the optical depth to Thompson scattering, goes a long way in enhancing the number of Pop III stars and dwarf galaxies with halo masses $M_{halo} < 10^8 M_\odot$ that can only form before IGM reheating and reionization at redshift $z \sim 6\text{--}10$. The maximum number of Pop III stars is obtained when the critical halo mass in which gas can cool in less than a Hubble time equals the Jeans mass of the IGM. This happens for $K_X = 0.01 K_{LW}^{0.5}$, where K_X and K_{LW} are the mean energies of the first sources of light in the soft X-ray and Lyman-Werner bands in units of 6×10^{53} ergs, respectively.

This low level of X-ray emission does not require assumptions on the presence of unknown X-ray sources such as IMBH or miniquasars: it is necessarily produced by SN explosions and SN remnants of Pop III stars, thus is an unavoidable consequence of Pop III star formation with a top heavy IMF (unless most stars are more massive than

$250 M_\odot$, that would lead to direct collapse into black holes without SN explosion). In addition, if a non-negligible fraction of Pop III stars explode as hypernovae or PISNe, the soft X-rays from their remnants and explosions is sufficiently large to promote the formation of Pop III stars to about 400 per cMpc^3 , that is near the maximum number of Pop III stars with typical masses $10\text{--}40 M_\odot$ that can form in any of our models with different K_X . A higher X-ray flux than the one provided by Pop III hypernovae, for instance produced by accretion onto IMBH from Pop III stars and miniquasars, would suppress the number of Pop III stars because of the excessive heating of the IGM. We find that X-rays emitted by HMXRBs have a negligible effect in boosting the number of Pop III stars when compared to the soft X-ray emission from the first SN remnants.

The implications of a large number of Pop III stars include: i) a copious production of black holes with masses similar to the ones detected by LIGO ($\sim 10\text{--}30 M_\odot$) via gravitational wave emission (Abbott et al. 2016) (about 10^4 BHs remnants of Pop III stars are estimated within the Milky Way in the hypernova scenario); ii) would provide super-massive black holes seeds; iii) although Pop III stars cannot fully reionize the IGM due to their bursty nature, they can contribute to the reionization process in a manner similar to an early X-ray background (Hartley & Ricotti 2016); iv) finally, since the mean distance between minihalos hosting Pop III stars is small ($n_{pop3}^{-1/3} \sim 13$ kpc physical at $z \sim 10$), it is easier for the metals ejected by their SN remnants to fill rather uniformly the IGM. A low-level metal pre-enrichment of the IGM (*i.e.*, the metallicity floor often assumed in zoom simulations of galaxy formation), promotes the formation of pre-reionization dwarf galaxies and increases the number of their fossil relics in the Local Group (Ricotti & Gnedin 2005; Bovill & Ricotti 2009). The population of ultra-faint dwarfs discovered since 2005 orbiting the Milky Way (Belokurov et al. 2007; Drlica-Wagner et al. 2015; Koposov et al. 2015) is indeed consistent with a large population of pre-reionization dwarf galaxies (Bovill & Ricotti 2011a,b).

ACKNOWLEDGMENTS

I would like to thank the anonymous reviewer for the positive feedback and helping to improve the presentation of the material in the manuscript. MR acknowledges support from NSF CDI-typeII grant CMMI1125285 and the Theoretical and Computational Astrophysics Network (TCAN) grant AST1333514.

APPENDIX A: FITS TO PRESS-SCHECHTER

We use a modified Schechter equation to describe the dark matter mass function of minihalos obtained from the Press-Schechter formalism (including the Sheth-Tormen modification):

$$n_{halo}(M, z) = 3.98 \times 10^{10} (M/0.1)^{-\alpha} \exp[-(M/M_*)^{0.33}], \quad (A1)$$

where n_{halo} is the number of minihalos per unit $\ln M$ bin. Fits to the faint-end slope $\alpha = 1.05 + 0.029(z1 - 7.8)$, and the truncation mass $\log(M_*) = 8.8 - 0.165(z1 - 7.8)$, are given as a function of redshift z for Planck cosmological parameters.

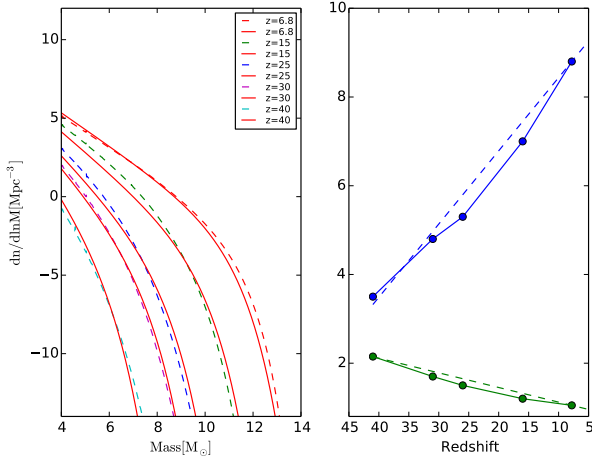


Figure A1. (Left) Mass function of dark matter halos from Press-Schechter formalism (solid lines) and fitting functions (dashed lines) from Equation (A1). The redshifts (Right) Fitting parameters α (green line) and M_* (blue line) as a function of redshift.

In Figure A1 are shown the the mass functions using Press-Schechter formalism compared to the fitting function (left panel), and the fitting parameters α and M_* as a function of redshift.

APPENDIX B: RATES

In this appendix we summarize the rates used in our model. We adopt the H_2 cooling rate $\Lambda(T)$ [$\text{erg cm}^3 \text{s}^{-1}$] from (Galli & Palla 1998):

$$\log(\Lambda(T)) = -103.0 + 97.59 \log(T) - 48.05 \log(T)^2 \quad (\text{B1})$$

$$+ 10.80 \log(T)^3 - 0.9032 \log(T)^4 \quad (\text{B2})$$

The H^- formation rate and the H_2 dissociation rates are respectively (Cazaux & Spaans 2004),

$$k_1 = 1.4 \times 10^{-18} T^{0.928} \exp(-T/16200.0) \quad (\text{B3})$$

$$k_2 = \max(3.3 \times 10^{-11} G_{\text{LW}}, t_H^{-1}). \quad (\text{B4})$$

The effect of secondary ionizations from photoelectrons is described by the following functions (Shull & van Steenberg 1985; Valdés & Ferrara 2008)

$$f_h = 1 - 0.8751(1 - x_e^{0.4}) \quad (\text{B5})$$

$$f_i = 0.3846(1 - x_e^{0.54})^{1.19}, \quad (\text{B6})$$

where f_h is the fraction of fast photoelectrons that is thermalized and f_i the fraction that produce secondary ionizations.

REFERENCES

Abbott, B. P., et al. 2016, Physical Review Letters, 116, 061102
 Abel, T., Bryan, G. L., & Norman, M. L. 2002, Science, 295, 93
 Belokurov, V., et al. 2007, ApJ, 654, 897

Bovill, M. S., & Ricotti, M. 2009, ApJ, 693, 1859
 Bovill, M. S., & Ricotti, M. 2011a, ApJ, 741, 17
 Bovill, M. S., & Ricotti, M. 2011b, ApJ, 741, 18
 Bromm, V., Coppi, P. S., & Larson, R. B. 1999, ApJ, 527, L5
 Bromm, V., Ferrara, A., Coppi, P. S., & Larson, R. B. 2001, MNRAS, 328, 969
 Cazaux, S., & Spaans, M. 2004, ApJ, 611, 40
 Christensen, C., Quinn, T., Governato, F., Stilp, A., Shen, S., & Wadsley, J. 2012, MNRAS, 425, 3058
 Drlica-Wagner, A., et al. 2015, ApJ, 813, 109
 Fragos, T., Lehmer, B. D., Naoz, S., Zezas, A., & Basu-Zych, A. 2013, ApJ, 776, L31
 Galli, D., & Palla, F. 1998, A&A, 335, 403
 Gnedin, N. Y., & Kravtsov, A. V. 2010, ApJ, 714, 287
 Haardt, F., & Madau, P. 2012, ApJ, 746, 125
 Haiman, Z., Abel, T., & Rees, M. J. 2000, ApJ, 534, 11
 Hartley, B., & Ricotti, M. 2016, ArXiv e-prints
 Heger, A., & Woosley, S. E. 2002, ApJ, 567, 532
 Helgason, K., Ricotti, M., Kashlinsky, A., & Bromm, V. 2015, ArXiv e-prints
 Hopkins, P. F., Kereš, D., Oñorbe, J., Faucher-Giguère, C.-A., Quataert, E., Murray, N., & Bullock, J. S. 2014, MNRAS, 445, 581
 Jeon, M., Bromm, V., Pawlik, A. H., & Milosavljević, M. 2015, MNRAS, 452, 1152
 Jeon, M., Pawlik, A. H., Bromm, V., & Milosavljević, M. 2014, MNRAS, 440, 3778
 Koposov, S. E., Belokurov, V., Torrealba, G., & Evans, N. W. 2015, ApJ, 805, 130
 Kuhlen, M., Madau, P., & Krumholz, M. R. 2013, ApJ, 776, 34
 Lopez, L. A., Ramirez-Ruiz, E., Huppenkothen, D., Badenes, C., & Pooley, D. A. 2011, ApJ, 732, 114
 Machacek, M. E., Bryan, G. L., & Abel, T. 2003, MNRAS, 338, 273
 Mapelli, M., Ferrara, A., & Pierpaoli, E. 2006, MNRAS, 369, 1719
 Muratov, A. L., Gnedin, O. Y., Gnedin, N. Y., & Zemp, M. 2013, ApJ, 772, 106
 Oh, S. P. 2001, ApJ, 553, 499
 Park, K., & Ricotti, M. 2011, ApJ, 739, 2
 Park, K., & Ricotti, M. 2012, ApJ, 747, 9
 Park, K., & Ricotti, M. 2013, ApJ, 767, 163
 Planck Collaboration, et al. 2015, ArXiv e-prints
 Ricotti, M. 2009, MNRAS, 392, L45
 Ricotti, M., & Gnedin, N. Y. 2005, ApJ, 629, 259
 Ricotti, M., Gnedin, N. Y., & Shull, J. M. 2001, ApJ, 560, 580
 Ricotti, M., Gnedin, N. Y., & Shull, J. M. 2002a, ApJ, 575, 33
 Ricotti, M., Gnedin, N. Y., & Shull, J. M. 2002b, ApJ, 575, 49
 Ricotti, M., Gnedin, N. Y., & Shull, J. M. 2008, ApJ, 685, 21
 Ricotti, M., & Ostriker, J. P. 2004, MNRAS, 352, 547
 Ricotti, M., Ostriker, J. P., & Gnedin, N. Y. 2005, MNRAS, 357, 207
 Ricotti, M., Ostriker, J. P., & Mack, K. J. 2008, ApJ, 680, 829
 Robertson, B. E., Ellis, R. S., Furlanetto, S. R., & Dunlop, J. S. 2015, ApJ, 802, L19

- Shull, J. M., & van Steenberg, M. E. 1985, *ApJ*, 298, 268
- Stacy, A., Greif, T. H., & Bromm, V. 2010, *MNRAS*, 403, 45
- Steidel, C. C., Hunt, M. P., Shapley, A. E., Adelberger, K. L., Pettini, M., Dickinson, M., & Giavalisco, M. 2002, *ApJ*, 576, 653
- Tassis, K., Gnedin, N. Y., & Kravtsov, A. V. 2012, *ApJ*, 745, 68
- Tegmark, M., Silk, J., Rees, M. J., Blanchard, A., Abel, T., & Palla, F. 1997, *ApJ*, 474, 1
- Thompson, R., Nagamine, K., Jaacks, J., & Choi, J.-H. 2014, *ApJ*, 780, 145
- Turk, M. J., Abel, T., & O’Shea, B. 2009, *Science*, 325, 601
- Umeda, H., & Nomoto, K. 2003, *Nature*, 422, 871
- Valdés, M., & Ferrara, A. 2008, *MNRAS*, 387, L8
- Venkatesan, A., Giroux, M. L., & Shull, J. M. 2001, *ApJ*, 563, 1
- Wheeler, C., Onorbe, J., Bullock, J. S., Boylan-Kolchin, M., Elbert, O. D., Garrison-Kimmel, S., Hopkins, P. F., & Keres, D. 2015, *ArXiv e-prints*
- Wise, J. H., & Abel, T. 2008, *ApJ*, 685, 40
- Wise, J. H., Demchenko, V. G., Halicek, M. T., Norman, M. L., Turk, M. J., Abel, T., & Smith, B. D. 2014, *MNRAS*, 442, 2560
- Xu, H., Ahn, K., Wise, J. H., Norman, M. L., & O’Shea, B. W. 2014, *ApJ*, 791, 110